Korean J. Chem. Eng., 39(7), 1753-1761 (2022)
DOI: 10.1007/s11814-022-1079-2

pISSN: 0256-1115
eISSN: 1975-7220

Design of low-loaded NiRe bimetallic catalyst on N-doped mesoporous carbon for highly selective deoxygenation of oleic acid to n-heptadecane

Zuojun Wei*,, Yuran Cheng*,**, Mengting Chen***, Yuhua Ye***, and Yingxin Liu***,†**

*Key Laboratory of Biomass Chemical Engineering of the Ministry of Education, College of Chemical and Biological Engineering, Zhejiang University, 38 Zheda Road, Xihu District, Hangzhou 310027, P. R. China
**Institute of Zhejiang University-Quzhou, 78 Jinhua Boulevard North, Quzhou 324000, P. R. China
***Research and Development Base of Catalytic Hydrogenation, College of Pharmaceutical Science, Zhejiang University of Technology, 18 Chaowang Road, Xiacheng District, Hangzhou 310014, P. R. China
(*Received 2 November 2021 • Revised 24 January 2022 • Accepted 27 January 2022*)

Abstract−Using nitrogen-doped mesoporous carbon (NMC) as the support, several NiRe bimetallic catalysts with low metal loading of 1 wt% were designed and prepared for the selective deoxygenation of oleic acid to n-heptadecane in the absence of hydrogen. Results showed that the $Ni_{80}Re_{20}$/NMC catalyst with a Ni/Re molar ratio of 80 : 20 achieved the highest yield of n-heptadecane (92.3%) at 330 °C for 2 h in isopropanol solvent, and at a metal/oleic acid weight ratio of 1 : 333. The catalyst can be reused at least five times with slight activity loss. Combined with the results of in-situ XRD, HRTEM, XPS and CO_2-TPD, the formation of NiRe alloy, the very fine NiRe nanoparticle size at 2.30 nm, as well as the hydrophobic, mesoporous and weakly basic properties of the NMC support surface were demonstrated to contribute to the excellent catalytic performance of the catalyst.

Keywords: Oleic Acid, Deoxygenation, Hydrogen Donor, NiRe Bimetallic Catalyst, Nitrogen-doped Mesoporous Carbon

INTRODUCTION

The removal of oxygen from fatty acids to form paraffinic hydrocarbons has been attracting considerable attention to the conversion of biomass for the direct replacement of traditional petroleum-derived liquid transportation fuels [1,2]. For saturated fatty acids, such a deoxygenation process could be easily accomplished through decarboxylation or decarbonylation reaction with considerably high yield over kinds of catalysts [3,4]. For unsaturated fatty acids, however, things become a bit complex due to the existence of C=C bonds. In this regard, one apparent strategy is a two-step process: the hydrogenation of unsaturated C=C bonds followed by the deoxygenation reaction, which is technically feasible but inevitably deserves criticism for tedious steps and the consumption of another cleaner fuel of hydrogen [5,6]. Another more concise and highly concerned strategy is the direct deoxygenation of unsaturated fatty acids in absence of hydrogen. Unfortunately, the development of an efficient catalytic system for this process is more challenging than that for saturated fatty acids.

The main target of the present work was to design an effective catalytic system for the deoxygenation of oleic acid to n-heptadecane in absence of hydrogen. To reach this goal, three aspects were considered for designing a catalyst. The primary thing is the selection of the main active metallic component. Although noble metals exhibit excellent performance for deoxygenation of saturated stearic acid, they fail to deal with deoxygenation of unsaturated oleic acid. For example, Pd was viewed as one of the most effective metals for the deoxygenation of stearic acid, with a yield of n-heptadecane exceeding 95% [7,8]. However, given oleic acid as the substrate, the n-heptadecane yield was only 2-26% [8-10]. For Pt/C catalyst, the highest yield of n-heptadecane from deoxygenation of oleic acid in absence of hydrogen was achieved at 71% [11], yet a much lower yield of n-heptadecane (<18%) was also reported in similar reaction conditions [12]. In contrast, more than 90% of corresponding paraffins could be obtained while saturated fatty acids were used as starting materials over Pt-based catalysts [13]. Similar to Pt and Pd, most Ni-based catalysts are only active for deoxygenation of saturated stearic acid, or dealing with oleic acid in presence of hydrogen [3,14], except for the newly developed Cu-Ni catalysts [15-17], which obtained n-heptadecane yields of 91.3%-92.7% from the deoxygenation of oleic acid using methanol, water or isopropanol as hydrogen donors. However, one obvious drawback of those Cu-Ni catalysts is that the metal loading is as high as 30-60 wt%. Consequently, the initial ratios of oleic acid to metals were only 4.7-7.8 (w/w), indicating a relatively low catalytic efficiency. This is generally reasonable: compared to Pt and Pd, base metals such as Fe, Co, Ni or Cu are viewed as less active and a higher metal loading is always necessary to reach the desired activity [3,18,19]. On the other hand, it is well known that lower metal loading tends to result in smaller metal nanoparticles, better particle distribution, and higher metal dispersion, as well as more angle and edge portion of metal atoms which are believed to be more catalytically active [14,20,21]. We therefore speculate that low Ni loading may be a better choice for the deoxygenation of unsaturated fatty acids.

Actually, it is expected that high n-heptadecane yield for the deoxygenation of oleic acid could not be obtained over single Ni cata-

†To whom correspondence should be addressed.
E-mail: yxliu@zjut.edu.cn

lysts, as none of the reported pure Ni- or Co-based catalysts obtained a n-heptadecane yield exceeding 10% [22,23]. An alternative strategy is to modify Ni with a second metal to form a bimetallic catalyst, which is quite popular in deoxygenation of fatty acids [22,24]. Herein, we chose Re as the second metal to evaluate the synergistic effect of NiRe bimetallic catalysts for deoxygenation of unsaturated fatty acids/oleic acid.

The third consideration for designing the catalyst is the selection of an ideal support. Since oleic acid and most of the other unsaturated fatty acids appearing in natural fatty esters have long carbon chains and therefore are quite hydrophobic, the conventional porous hydrophilic supports, such as SiO_2, γ-Al_2O_3, CeO_2, zeolite 5A and hydrotalcite, if used as a catalyst support, may bring diffusion problems due to the polarity discrepancy between substrate and support [25]. Hence, hydrophobic carbon materials, such as activated carbon (AC) and carbon nanotube, might be better choices. The newly developed mesoporous carbon (MC) with pore size distribution mainly between 4-10 nm [26,27] is also a promising alternative catalyst support for deoxygenation of fatty acids. Apart from the hydrophobic and mesoporous structure, which is better accessible to the active sites of the substrates, MC takes the advantage of being easily modified with heteroatoms or functional groups to obtain desired physicochemical properties. Modification of MC with nitrogen is generally viewed as an effective way to improve the size distribution dispersion of the metals supported on and increase the stability of the catalysts [28,29]. More importantly, it is expected that the weak basicity of nitrogen heteroatom may be an active site to selectively adsorb carboxyl groups in fatty acids to the vicinity of metal nanoparticles supported on the MC surface, and in the end improve the catalytic performance of the catalyst. In our previous work, we synthesized nitrogen-doped mesoporous carbon (NMC) by a dual-templating approach employing tetraethyl orthosilicate as hard template, Pluronic F127 as soft template, and melamine-phenol-formaldehyde (MPF) resin as both carbon and nitrogen precursors. The NMC supported Pt and Ru catalyst exhibited high activity and recyclability in deoxygenation of saturated fatty acids and other bio-transformation reactions [13,27]. In the present paper, we report that NMC supported NiRe bimetallic catalyst with low metal loading of 1 wt% is an effective heterogeneous catalyst for the deoxygenation of oleic acid to n-heptadecane.

EXPERIMENTAL

1. Materials

$Ni(NO_3)_2{\cdot}6H_2O$ and NH_4ReO_4 were purchased from Shanghai Jiuling Chemical Co. Ltd., China. Oleic acid was purchased from Aladdin Co. Ltd., China. Activated carbon was purchased from Xinsen Carbon Co, China. Other chemicals were purchased from Sinopharm Chemical Reagent Co. Ltd., China. All the chemicals were analytical grade and used without further purification.

2. Catalyst Preparation

The NMC material was prepared following the same method as our previous work [13]. All the catalysts supported on various supports such as NMC, AC, SiO_2, γ-Al_2O_3 and TiO_2 were prepared by incipient wetness impregnation method. For each mono- or bimetallic catalyst, the total metal loading was fixed at 1 wt% with respect to the support, and the molar ratio of the two metals may be altered for the bimetallic catalysts. In a typical procedure for preparing 1 wt% NiRe/NMC catalyst with a Ni/Re molar ratio of 1 : 1, 0.0594 g of $Ni(NO_3)_2{\cdot}6H_2O$ and 0.0548 g of NH_4ReO_4 were dissolved in ca 5.32 g of double-distilled water and then slowly added to 4.95 g of NMC support at room temperature. After being impregnated for 24 h, the mixture was vacuum dried at 110 °C for 10 h and finally reduced at 500 °C in a tubular furnace under hydrogen flow for 4 h to obtain the target catalyst, which was denoted as $Ni_{50}Re_{50}$/NMC (the subscripts denote that the molar ratio of Ni/Re is 50 : 50).

3. Catalyst Characterization

X-ray powder diffraction (XRD) patterns were recorded with an XRD-600 diffractometer (Shimadzu Co., Japan) using a Cu Kα radiation (λ=0.15406 nm) in a Bragg-Brentano parafocusing optics configuration (40 kV, 40 mA). Samples were scanned from 10 to 80° with a scanning rate of 4° min^{-1} and a step size of 0.02°. The crystalline phases were identified by reference to the JCPDS database. The *in-situ* XRD patterns of the catalyst were recorded under a flow of H_2 (30 ml·min^{-1}) during the stepwise heating of the sample from 25 to 500 °C at the rate of 5 °C·min^{-1}.

Transmission electron microscopy (TEM) and high-angle annular dark-field scanning TEM (HAADF-STEM) images were obtained using a TecnaiG2F30 S-Twin instrument (FEI Co., USA) operated at an accelerating voltage of 300 kV. A probe-corrected transmission electron microscopy (Titan G2 80-200 ChemiSTEM, FEI) was applied for deep analysis of the structure of the NiRe alloy. This instrument incorporates the function of spherical aberration corrector and ChemiSTEM technology. The acceleration voltage was set to 80 kV to alleviate specimen damage induced by beam radiation. The probe current and convergence angle were set as 70 pA and 22 mrad, respectively. Under such conditions, the resolution achieved for HAADF-STEM image is estimated to be 0.08 nm, which is much more accurate than 0.25 nm of the former TEM microscope. Samples for both microscopes were prepared by dispersing the catalyst powder in ethanol under ultrasound for 15-20 min and then dropping the suspension onto a copper grid coated with carbon film. Particle size distribution of metal nanoparticles in the sample was determined from the corresponding STEM image by measuring the sizes of more than 200 particles.

Brunauer-Emmett-Teller (BET) specific surface areas and pore structures were measured by pulsed nitrogen adsorption-desorption method at −196 °C using an ASAP 2010 instrument (Micromeritics Instrument Co.). Prior to N_2 physisorption, the samples were degassed under vacuum at 250 °C overnight. The specific surface area was calculated by using the Brunauer-Emmett-Teller (BET) method, and the pore size distribution and pore volume were measured by Barrett-Joyner-Halenda (BJH) analysis from the adsorption branch of the isotherms.

X-ray photoelectron spectroscopy (XPS) spectra were obtained using an Escalab Mark II X-ray spectrometer (VG Co., United Kingdom) equipped with a magnesium anode (Mg Kα=1,253.6 eV), 50 eV pass energy, a 0.2 eV kinetic energy step, and 0.1 s dwelling time. Energy corrections were performed using a 1s peak of the pollutant carbon at 284.6 eV. The sample was prepared by pressing the catalyst powder onto the surface with silver sol gel.

Ni content was verified by atomic adsorption spectroscopy (AAS)

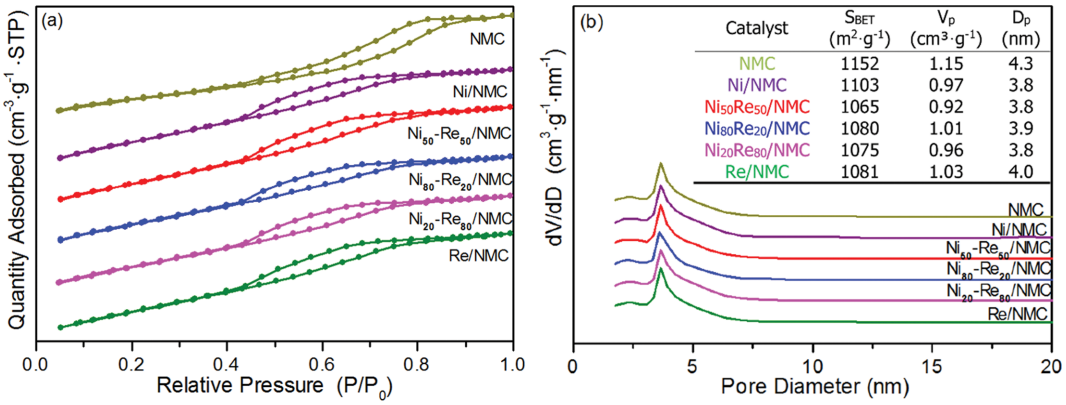

Fig. 1. (a) Nitrogen adsorption-desorption isotherms and (b) BJH pore size distributions of NMC and its supported catalysts with inset specific surface area (S_{BET}) $m^2 \cdot g^{-1}$, average pore volume (V_p) $cm^3 \cdot g^{-1}$ and average pore radius (D_p) nm.

method using a Varian AA 240 FS atomic adsorption spectrophotometer (AAS; Varian, Inc., USA). Re metal content was determined by ICP-MS (using a PerkinElmer Elan 9000 ICP Mass Spectrometer). The samples were first vacuum evaporated to remove organic solvent and then digested in a microwave digester using concentrated HNO_3 acid prior to AAS or ICP-MS analysis.

4. Reaction Procedure

Deoxygenation reaction of oleic acid was conducted in 1.67 ml unstirred mini-batch reactors assembled from 3/8-inch stainless steel Swagelok parts, the same as our previous work [13]. Prior to being used, the reactor was rinsed with acetone, followed by washing with water at 300 °C for 30 min to remove any residual materials. In a typical experiment, 15 mg of catalyst together with 50 mg of oleic acid and 1 ml of solvent was added into the reactor. The reactor was then sealed and immersed into a sand bath with the desired temperature to initiate the reaction. After the reaction, the reactor was taken out from the sand bath, cooled in a water bath to room temperature immediately, and sampled for GC analysis. No H_2 was added to the reactors in each entry of these reactions.

To minimize the experimental error brought from the change of the mini-reactors for different batches, each reaction entry was repeated at least three times, and we reported the data as an averaged value with an error range.

The reaction products were analyzed by using an Agilent 7890 gas chromatograph equipped with an HP-5 capillary column (30.0 m× 0.32 mm×0.25 μm) and a flame ionization detector (FID). Naphthalene was used as an interior standard for accurate quantification of oleic acid, octadecane and n-heptadecane. The correction factors to naphthalene were detected as 0.98, 1.02 and 1.03, respectively.

Product identification was performed with an Agilent 6890 gas chromatography system coupled to a mass spectrometer equipped with an Agilent 5973 quadrupole mass analyzer. The typical GC and MS diagrams of the components are listed in Fig. S1.

RESULTS AND DISCUSSION

1. Catalyst Characterization

The physicochemical property and morphological structure of the NiRe/NMC catalysts were characterized. The nitrogen physisorption properties of NMC and NMC supported mono- and bimetallic catalysts are summarized in Fig. 1. The BET specific surface areas, pore volumes and pore sizes are in the range of 1,065-1,152 $m^2 \cdot g^{-1}$, 0.92-1.15 $cm^3 \cdot g^{-1}$, and 3.77-4.28 nm, respectively. Loading metal(s) on the NMC only slightly decreases these values.

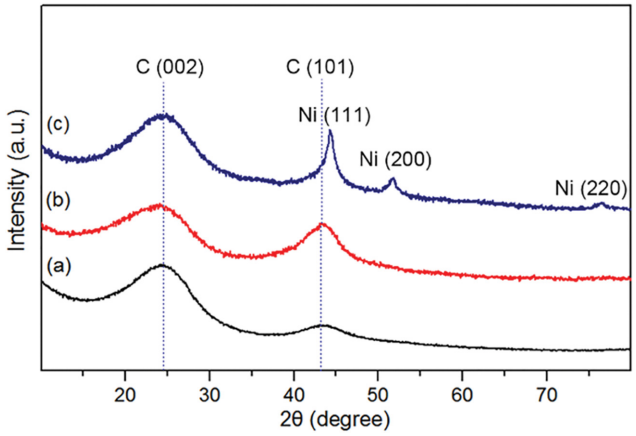

Fig. 2. XRD patterns of Ni and NiRe catalysts. (a) 1 wt% $Ni_{80}Re_{20}$/NMC, (b) 5 wt% $Ni_{80}Re_{20}$/NMC and (c) 4 wt% Ni/NMC. Prior to determination, the catalyst was reduced at 500 °C under hydrogen for 3 h.

The conventional XRD pattern for 1 wt% $Ni_{80}Re_{20}$/NMC catalyst shows only two broad diffraction peaks at 2θ=23° and 43.5° (Fig. 2), which are generally recognized as C (002) and C (101) of MC materials [27,30]. No significant signals attributed to Ni, Re or NiRe species were observed, indicating that metal particles on NMC surface were too small to be detected by XRD. We intentionally increased the total metal loading to 5 wt% with the same Ni/Re molar ratio to check whether the signals of metals were too low to be discriminated and observed similar diffraction pattern except for the enhancement of the C (101) peak. However, the monometallic Ni/NMC catalyst with the same Ni loading of 4 wt% shows obvious Ni (111), Ni (200) and Ni (220) diffraction peaks (2θ=44.5, 51.9 and 76.5°) [22,31]. The results indicate that the addi-

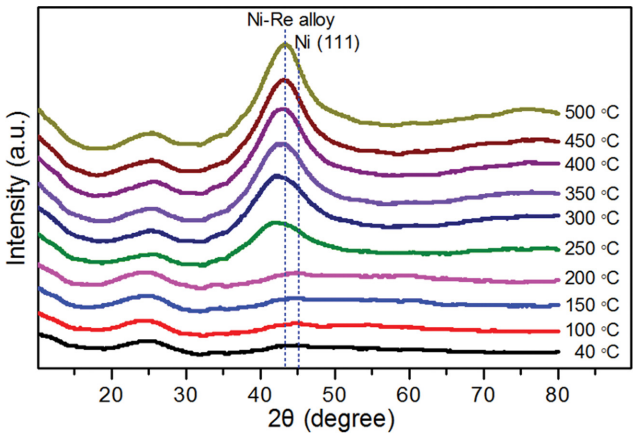

Fig. 3. In-situ XRD patterns for 5 wt% $Ni_{80}Re_{20}$/NMC at temperatures ranging from 40 to 500 °C.

tion of Re totally changed the crystalline of Ni. Since the diffraction signal of metals in 1 wt% $Ni_{80}Re_{20}$/NMC is too weak to be recognized, and considering that higher loading of metal mixtures would not alter the crystal structure but only the nanoparticle size, we applied *in situ* XRD patterns for 5 wt% $Ni_{80}Re_{20}$/NMC precursor instead of 1 wt% loading catalyst at temperatures ranging from 40 to 500 °C (Fig. 3). It can be seen that only one main strong and board diffraction peak at 2θ=43.5° was formed when the temperature was over 250 °C, which is 1° less than that of Ni (111) (2θ=4.5°), indicating the formation of NiRe alloy [32].

The TEM (Fig. 4(a)) and HAADF-STEM (Fig. 4(b)) images of the 1 wt% $Ni_{80}Re_{20}$/NMC catalyst show that the metal nanoparticles are well dispersed with a very fine particle size of 2.30±0.35 nm, which is in accordance with the broad diffraction peak in the XRD pattern (Fig. 2). Only a fringe spacing of 0.23 nm (inset in Fig. 4(a)) was observed in the catalyst, which may be ascribed to a Miller

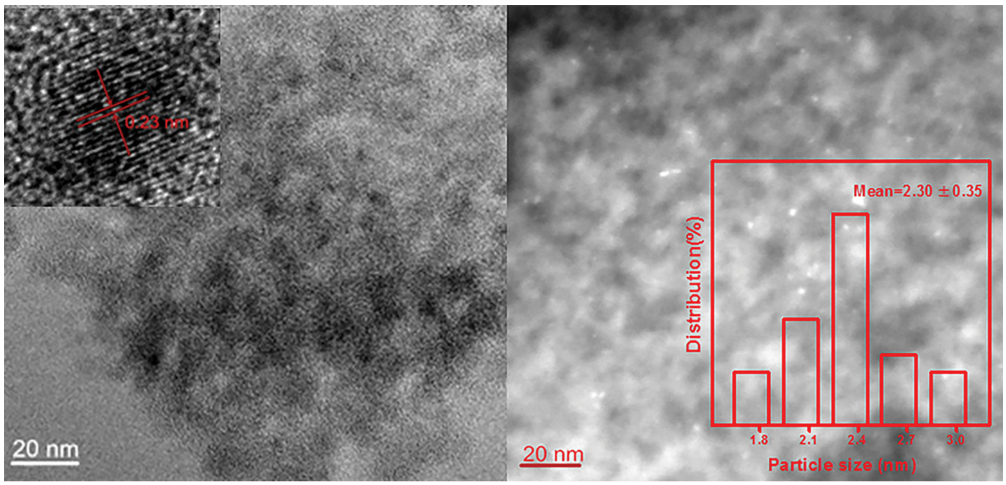

(a) **(b)**

Fig. 4. (a) TEM and (b) HAADF-STEM images of 1 wt% Ni_{80}-Re_{20}/NMC catalyst with inset the corresponding size distribution of NiRe nanoparticles.

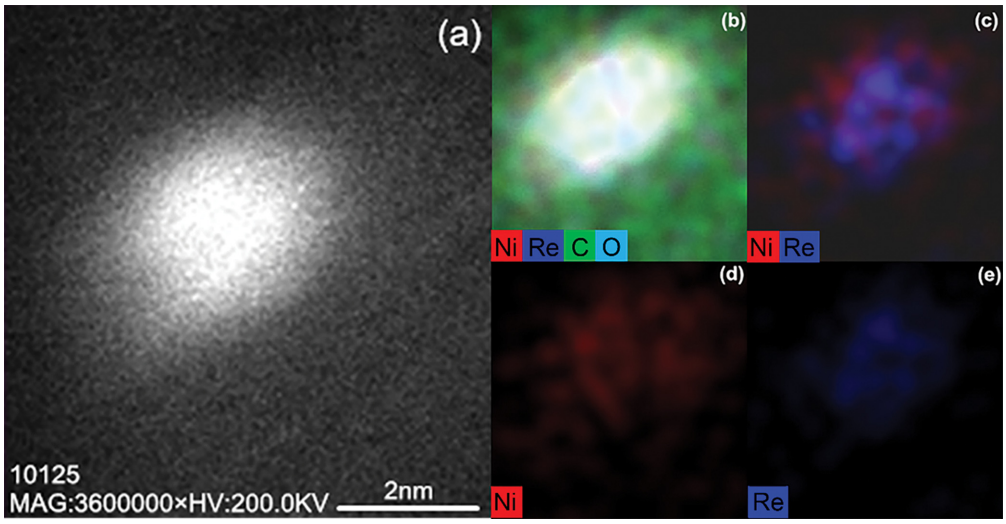

Fig. 5. (a) High-resolution HAADF-STEM image and (b)-(e) elemental mappings of NiRe nanoparticles on 1 wt% Ni_{80}-Re_{20}/NMC catalyst by a probe-corrected TEM.

surface of the newly formed alloy. It is not possible to obtain a stable elemental mapping of NiRe nanoparticles in such a conventional TEM microscope as we have used [19] due to the very fine size of the particles. We therefore turned to a more accurate probe-corrected TEM, which is three times higher in resolution than the former. As shown in Fig. 5, Ni and Re are homogenously mixed as an alloy in the particle core while Ni seems richer in the outer shell. N and O are distributed over the sample. Actually, in the metal particle range, O matches Re fairy well, indicating the existence of Re oxides.

The XPS spectra of 1 wt% Ni/NMC, 1 wt% Re/NMC and 1 wt% $Ni_{80}Re_{20}$/NMC catalysts were conducted to investigate the element composition and their electronic states on the catalyst surface. The Ni 2p spectra are shown in Fig. 6(a), with the expected doublets for Ni $2p_{1/2}$ and $2p_{3/2}$. The most intense peak pair at 854.5 and 872.0 eV in $Ni_{80}Re_{20}$/NMC catalyst is assigned to Ni (+2), occupying ca 42% of the total Ni element (Table S1). The second peak pair at 852.1 and 869.6 eV in $Ni_{80}Re_{20}$/NMC catalyst can be assigned to Ni (0) [33], occupying ca 9% of Ni element. The peak pair at 860.5 and 878.0 eV in the $Ni_{80}Re_{20}$/NMC catalyst is generally considered as the satellite peaks of Ni (+2), occupying ca 49% of Ni element [34], which may be due to the oxidation of Ni during preservation in air atmosphere, as being frequently reported for other Ni and Ni alloyed catalysts [31,35]. In general, Re exhibits a mixture of 0, +2, +3, +4, +6 and +7 valences when alloyed with Pd, Pt, Ir and Sn elements [36-40]. As shown in Fig. 6(b), binding energy in the range of 39-51 eV belongs to Re 4f region, which is deconvoluted into doublet peaks for $4f_{5/2}$ and $4f_{7/2}$ orbits, implying the presence of metallic Re ($4f_{5/2}$=42.7 eV, $4f_{7/2}$=40.3 eV), Re_2O_3 ($4f_{5/2}$=43.7 eV, $4f_{7/2}$=41.3 eV), and ReO_3 ($4f_{5/2}$=47.6 eV, $4f_{7/2}$=45.1 eV) [36,40-43] with the approximate atomic ratio of 26 : 18 : 56 in the $Ni_{80}Re_{20}$/NMC catalyst (Table S1). Compared to their monometallic counterparts, the binding energies of Ni species shift to higher values by ca 0.3 eV, while the binding energies of Re species decrease to lower values by ca 0.3 eV, indicating that strong interactions may exist between Ni and Re species through the formation of the alloy. In addition, the content of the metallic Re in the $Ni_{80}Re_{20}$/NMC catalyst increases by 14% (Table S1), and the higher valence of Re (+4) disappears compared to that in Re/NMC, indicating that the coexistence of nickel is conducive to the formation of metallic Re, which is in agreement with other reports [37,38].

2. Activity Test

The deoxygenation of oleic acid was conducted over 1 wt% NiRe bimetallic catalysts with various Ni/Re ratios. Isopropanol was used as both solvent and hydrogen donor. Two main products, n-heptadecane and octadecane, were concerned in our research. To our

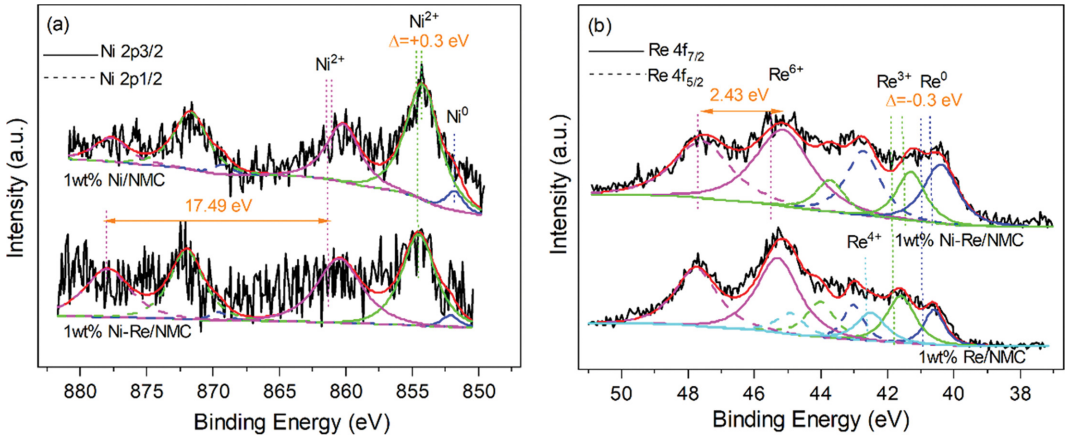

Fig. 6. XPS of 1 wt% $Ni_{80}Re_{20}$/NMC, 1 wt% Ni/NMC and 1 wt% Re/NMC catalysts in (a) Ni 2p and (b) Re 4f regions.

Table 1. Deoxygenation of oleic acid over different 1 wt% NiRe bimetallic catalysts

Entry	Catalyst	Conversion (%)	N-heptadecane yield (%)	Octadecane yield (%)
1	Re/NMC	>99	8.68±0.5	10.7±0.7
2	$Ni_{20}Re_{80}$/NMC	>99	62.4±1.3	21.1±1.1
3	$Ni_{50}Re_{50}$/NMC	>99	79.2±2.4	10.9±0.70
4	$Ni_{80}Re_{20}$/NMC	>99	92.3±2.5	4.85±0.50
5	Ni/NMC	90.5±2.7	20.7±1.0	2.24±0.25
6	NMC	81.8±1.6	<0.1	<0.1
7	$Ni_{50}Re_{50}/\gamma$-Al_2O_3	60.0±1.8	33.5±1.5	1.19±0.10
8	$Ni_{50}Re_{50}/SiO_2$	93.0±2.8	47.1±1.7	2.95±0.10
9	$Ni_{50}Re_{50}/TiO_2$	>99	36.7±1.5	0.50±0.10
10	$Ni_{50}Re_{50}$/AC	>99	60.4±1.5	6.42±0.30

Reaction conditions: oleic acid, 50 mg; isopropanol, 1 ml; catalyst, 15 mg; reaction temperature, 330 °C; reaction time, 2 h.

great excitement, the NiRe/NMC catalysts we designed in this work exhibited excellent performance for the deoxygenation of oleic acid to n-heptadecane. As shown in Table 1, NiRe/NMC bimetallic catalysts with Ni/Re molar ratios of 20 : 80, 50 : 50 and 80 : 20 (entries 2-4) showed obviously higher activity and selectivity to n-heptadecane than Re/NMC (entry 1) and Ni/NMC (entry 5) monometallic catalysts and bare NMC support (entry 6), indicating that there was a positive synergistic effect between Ni and Re on the deoxygenation reaction. Moreover, n-heptadecane yield increased with the increase in Ni/Re ratio and reached a maximum 92.3% at 80 : 20 of Ni/Re ratio (entry 4) under the pre-optimized reaction conditions: 330 °C of reaction temperature, 2 h of reaction time, and 1 : 333 of the metal/oleic acid weight ratio (Fig. S2). Considerable amounts of octadecane, another vital component of liquid fuels, were also observed. Thus, the maximum overall yield of n-heptadecane and octadecane reached 97.1% (entry 4). To the best of our knowledge, this is by far the highest yield of hydrocarbons from unsaturated fatty acids through deoxygenation in absence of hydrogen that has been ever reported. Since pure Re catalyst (entry 1) and bimetallic NiRe catalyst with higher content of Re tended to yield more octadecane, we deduce that Re prefers the production of octadecane, while Ni prefers the production of n-heptadecane.

To show the advantage of our NMC support, we also checked the performance of four other commercially available supports, i.e., γ-Al_2O_3, SiO_2, TiO_2 and AC supported NiRe catalysts (50 : 50 of Ni/Re molar ratio) for comparison (entries 7-10). As expected, all the three hydrophilic carriers supported NiRe catalysts, i.e., $Ni_{50}Re_{50}$/γ-Al_2O_3, $Ni_{50}Re_{50}/SiO_2$ and $Ni_{50}Re_{50}/TiO_2$, exhibited poor selectivity to either n-heptadecane or octadecane (less than 50%, entries 7-9), although 90-99% high conversions of oleic acid could also be obtained over SiO_2 and TiO_2 supported NiRe catalysts. The product analysis spectra were quite complex with around 30-50% of the products falling in the C_8-C_{18} range (Fig. S1), which seems more like pyrolysis than deoxygenation of oleic acid [44], indicating that the deoxygenation activity of NiRe catalyst was greatly suppressed due to the unavailability of hydrophobic oleic acid to the metal cites on the hydrophilic oxides surface. In contrast, over hydrophobic AC supported NiRe catalyst, the n-heptadecane yield of 60.4% (entry 10) is obviously higher than those of the oxide supports, but lower than that of NMC supported NiRe catalyst. Besides, proper solvent might also improve the yield of deoxygenation products by inhibiting such pyrolysis-like reaction of oleic acid (Table S3).

We further investigated the recyclability of the $Ni_{80}Re_{20}$/NMC catalyst for the deoxygenation of oleic acid to n-heptadecane. After reaction, the $Ni_{80}Re_{20}$/NMC catalyst was centrifuged, washed with isopropanol, and returned to the reactor for reuse. It can be seen from Fig. 7 that the catalyst could be reused at least five times with a slight decrease by ca 1.5% of oleic acid conversion and ca 4% of n-heptadecane yield at each run. Note that the weight loss of the catalyst during transferring contributed considerably to its activity loss due to its very small amount in the reaction (only 15 mg). Since metallic Ni as a catalyst is not recommended for acid substrate as it faces the risk of being oxidized to Ni (+2) [18], we further checked the Ni leaching during the reactions by determining the Ni concentrations in the reaction solutions through AAS. Besides, the Re concentrations in each cycle's reaction solution were also determined (Fig. 7). It can be seen that the Ni and Re concentrations in bulk solutions were around 35 $\mu g \cdot l^{-1}$ and 8 $\mu g \cdot l^{-1}$ during the five recycles, respectively, corresponding to 0.24% of Ni and 0.18% of Re in bulk catalyst, respectively, indicating that the formation of NiRe alloy would improve the stability of the Ni-based catalyst.

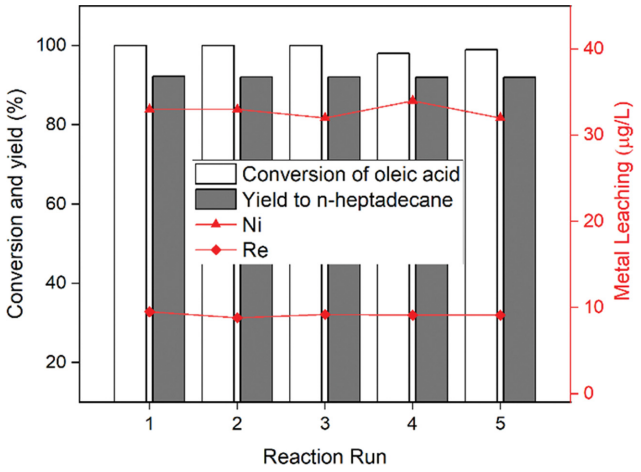

Fig. 7. Recyclability of $Ni_{80}Re_{20}$/NMC catalyst for deoxygenation of oleic acid. Reaction conditions: oleic acid, 50 mg; isopropanol, 1 ml; $Ni_{80}Re_{20}$/NMC catalyst, 15 mg; reaction temperature, 330 °C; reaction time, 2 h.

Hydrogen, either molecular state or atomic state, should be essential to saturate C=C bond in oleic acid to obtain n-heptadecane, octadecane and other saturated hydrocarbons. In addition to isopropanol, we evaluated formic acid, water, methanol, ethanol, and

Table 2. Deoxygenation of oleic acid over $Ni_{80}Re_{20}$/NMC catalyst in presence of different dual solvents and hydrogen donors

Entry	Hydrogen donor	$-\Delta_{red}H^0$ (kJ·mol^{-1})[a]	Conversion (%)	N-heptadecane yield (%)	Octadecane yield (%)
11	Formic acid	31.5	>99	28.25±0.4	49.5±1.5
12	Isopropanol	69.9	>99	92.3±2.5	4.85±0.5
13	Ethanol	85.4	>99	31.8±1.4	6.56±0.3
14	Methanol	130.6	>99	35.0±0.7	6.40±0.3
15	H_2O	239.2	61±3	27.9±0.9	0.30±0.10
16	*tert*-Butanol	-	>99	0 1.2±0.05	0.10±0.05

Reaction conditions: oleic acid, 50 mg; solvent, 1 ml; $Ni_{80}Re_{20}$/NMC catalyst, 15 mg; reaction temperature, 330 °C; reaction time, 2 h.
[a]Please also see Table S2 for better understanding on the reduction potential.

tert-butanol as atomic hydrogen donors for deoxygenation of oleic acid. As shown in Table 2, when using ethanol as a hydrogen donor, 31.8% of n-heptadecane yield obtained (entry 13), which is only one-third of that achieved in the case of isopropanol. When using the rest of the hydrogen donors tested in this work, the yield of n-heptadecane or octadecane was lower. For better understanding the hydrogen supplying ability of these hydrogen donors, a parameter of reduction potential $-\Delta_{red}H^0$ [45,46] was introduced (Table 2 and Table S2), which is defined as the difference in enthalpy of formation between a reductant and its corresponding oxidation state after delivery of two hydrogen atoms. A lower value of $-\Delta_{red}H^0$ corresponds to higher ability for delivering hydrogen atoms, and correlates well with hydrogen donors for obtaining higher yields of both n-heptadecane and octadecane. The only exception is formic acid, in which an unusual high octadecane yield of 49.5% was obtained (entry 11). This may be ascribed to the very strong reduction potential of formic acid that changed the deoxygenation pathway to the direct reduction of carboxyl group pathway [47]. *tert*-Butanol has no active hydrogen (no corresponding aldehyde/ketone as oxidation state), so it cannot be used as a hydrogen donor, and very low yields of n-heptadecane and octadecane were obtained (entry 16).

3. Discussion

Table 3 compares the catalysts which have been employed specifically for the deoxygenation of oleic acid in the absence of hydrogen. Among all these catalysts, our $Ni_{80}Re_{20}$/NMC catalyst with 1 wt% metal loading achieved the highest yield of n-heptadecane (92.3%), which is far higher than those catalyzed Pt, PtRe and PtSn noble metals/alloys (entries 18, 19, and 22) and comparable to the NiCu bimetallic catalysts (entries 24-26). The initial weight ratio of oleic acid to the total metal in our case is 333, which is much higher than that in most cases and comparable with the 5 wt% Pt/C (409, entry 18) and Pt-Re/C (769, entry 19) cases, showing the high efficiency of our catalyst. We have not yet evaluated our catalyst in the presence of hydrogen in this stage. Actually, according to the work from Yang et al. [25], who compared their Pt/zeolite 5A catalyst with other published catalysts for the deoxygenation of oleic acid in the presence of hydrogen, the highest yield of n-heptadecane was 72.6-81.5% (entry 23), which is also lower than the yield of 92.3% achieved by our $Ni_{80}Re_{20}$/NMC catalyst.

We believe that three factors may contribute to the excellent catalytic performance. First, the formation of NiRe alloy, which has been proven by the XRD, TEM and XPS results, would have a synergistic effect on the deoxygenation reaction, as it is believed that the addition of a second metal will form heteroatom bonds that change the electronic environment of the metal surface, and change the micro geometry of the metal lattice [50, 51]. In the NiRe alloy, Re is in the form of Re and ReO_x (Re_2O_3, ReO_3 and other Re oxides). Due to the high electronegativity of oxygen, Re is highly electron deficient, which will accept partial free electrons from metallic Ni in the alloy. As a result, the alloyed Ni catalyst is much more stable and shows higher recyclability. Moreover, the polar Re-O bond may also selectively attract hydroxyl group in oleic acid through hydrogen bond or static interactions, and therefore improve the deoxygenation reaction. A similar viewpoint has also been proved by recent quantum chemistry calculations and modern physical characterizations [52].

Second, the low metal loading of the $Ni_{80}Re_{20}$/NMC catalyst is beneficial to obtain high activity. In our work, the total loading of Ni and Re in our catalyst is only 1 wt%, which is much lower than Ni loadings in other ever reported Ni catalysts [4,18,22]. At such low loading of Ni and Re, the size of NiRe particles is only around 2 nm from TEM observation (Fig. 4), which is far smaller than the sizes in Ni-based catalysts having metal loadings more than 10 wt% (For example, 8-13 nm in our former NiFe alloy at 20 wt% loading on AC [18]). It is well known that lower metal loading and smaller metal nanoparticles always lead to more homogeneous particle distribution and higher metal dispersion because more metal atoms are exposed on the surface, and also lead to more angle and edge portion of metal atoms, which are believed to be more catalytically active [20,21]. On the other hand, the aggregation of the Ni nanoparticles was greatly inhibited due to the formation of NiRe alloy. As a consequence, the prepared NiRe catalyst is both active and stable. When Ni was used as a catalyst, people preferred a higher loading of Ni. This is probably because Ni is not as highly catalytically active as those noble metals. Besides, it is generally known that Ni is much easier to be oxidized than noble metals during preservation in air, and in turn it also needs a higher reduction temperature to reach metallic state than noble metals [52]. The oxidized Ni covering the metallic Ni further decreases the expo-

Table 3. Comparison of the conversion of oleic acid to n-heptadecane over different catalysts

Entry	Catalyst	Hydrogen donor	Oleic acid/Metal (w/w)	Conversion (%)	N-heptadecane yield (%)	Ref
17	Activated carbon	Water	-	80±4	6±1	[48]
18	5 wt% Pt/C	None	409	99.0	71.0	[11]
19	Pt-Re/C	Glycerol	769	92	37	[47]
20	30 wt% Ni/C	None	5.6	100	55.6	[49]
21	NiWC/Al-SBA-15	Water	44	30.7	0.72	[22]
22	Pt_3Sn/C	Water	113	100	60.0	[5]
23	Pt/zeolite 5A	Hydrogen	100	98.7	72.6±2	[25]
24	60 wt% CuNi/Al_2O_3	Methanol+water	5.6	100	92.7	[16]
25	30 wt% $Cu_{0.65}Ni_{0.35}/ZrO_2$	Methanol	11.1	100	92.5	[17]
26	50 wt% $Ni_{0.5}Cu_{0.5}$/CoOx	Isopropanol	4.7	99	91.3	[15]
27	1 wt%$Ni_{80}Re_{20}$/NMC	Isopropanol	333	>99	92.3±2.5	This work

sure of metallic Ni, leading to deactivation of the catalyst. This may be another important reason for the use of higher Ni loading in the traditional Ni-based catalysts. Bearing in mind the easier oxidation of Ni, we intentionally conducted each step for adding catalyst and other reactants to reactors in a glove box purged with nitrogen. Actually, in a control experiment the $Ni_{80}Re_{20}$/NMC catalyst was exposed to air overnight prior to use; the selectivity to n-heptadecane greatly decreased to 60% at the first run (data entry not shown).

Finally, the hydrophobic, mesoporous and weakly basic properties of the NMC support surface will promote the approaching of carboxyl group to the vicinity of metal active sites and accelerate the deoxygenation reaction in the end. As proved in our experiment, NMC support was more favorable to the deoxygenation of oleic acid than both hydrophilic supports and AC. Although AC is always criticized by the large portion of micropores, which brings diffusion problems to the substrates, its hydrophobic property is beneficial to the adsorption of hydrophobic carbon chain in oleic acid to the vicinity of metals, and in the end achieves satisfactory n-heptadecane yield. Compared with AC, NMC has larger portion of mesopores, which is beneficial to the mass transfer of reactants inside the catalyst. As a result, the NiRe catalysts exhibited the performance in the order of NiRe/NMC>NiRe/AC>NiRe/hydrophilic oxides. More importantly, similar to the interaction between Re-O bond and hydroxyl group, we believe that the weak basicity of nitrogen in NMC, demonstrated by the CO_2-TPD profiles of as-prepared NMC and commercial activated carbon (Fig. S3), which may selectively adsorb carboxyl group through hydrogen bond, also contributes to the higher catalytic performance of the catalyst.

CONCLUSIONS

We have designed NMC supported low-loaded NiRe bimetallic catalysts for the selective deoxygenation of oleic acid to n-heptadecane. Results show that the 1 wt% $Ni_{80}Re_{20}$/NMC catalyst achieved the highest yield of n-heptadecane (92.3%) at 330 °C within 2 h in isopropanol solvent, and at metal/oleic acid weight ratio of 1 : 333. *In-situ* XRD, HRTEM and XPS characterization showed that Ni alloyed with Re with a very fine nanoparticle size of 2.30±0.35 nm. The excellent catalytic performance of the NiRe bimetallic catalyst is mainly ascribed to the following three factors. First, the formation of NiRe alloy in the NiRe bimetallic catalyst, which changes the micro geometry of the metal lattice and forms heteroatom bonds that change the electronic environment of the metal surface. Second, the low metal loading resulted in very small NiRe particles in the catalyst, which is beneficial to obtaining a more homogeneous particle distribution and higher metal dispersion because more metal atoms are exposed on the catalyst surface, and also leads to more angle and edge portion of metal atoms, which are believed to be more catalytically active. Finally, the hydrophobic, mesoporous and weakly basic properties of the NMC support surface will promote the approaching of carboxyl group to the vicinity of metal active sites and accelerate the deoxygenation reaction in the end.

ACKNOWLEDGEMENTS

This work was supported by the National Natural Science Foundation of China [21878269 and 21476211]; and the Zhejiang Provincial Natural Science Foundation of China [LY16B060004 and LY18B060016]; and Jiangxi Qilin Chemical Industry Co., Ltd [YX-[2012]008@].

SUPPORTING INFORMATION

Additional information as noted in the text. This information is available via the Internet at http://www.springer.com/chemistry/journal/11814.

REFERENCES

1. Y. M. Isa and E. T. Ganda, *Renew. Sust. Enegr. Rev.*, **81**, 69 (2018).
2. X. Y. Yao, T. J. Strathmann, Y. L. Li, L. E. Cronmiller, H. L. Ma and J. Zhang, *Green Chem.*, **23**, 1114 (2021).
3. J. Zhong, Q. Deng, T. M. Cai, X. Li, R. Gao, J. Wang, Z. L. Zeng, G. P. Dai and S. G. Deng, *Fuel*, **292**, 9 (2021).
4. P. Kumar, S. R. Yenumala, S. K. Maity and D. Shee, *Appl. Catal. A: Gen.*, **471**, 28 (2014).
5. T. M. Yeh, R. L. Hockstad, S. Linic and P E. Savage, *Fuel*, **156**, 219 (2015).
6. V. Itthibenchapong, A. Srifa, R. Kaewmeesri, P. Kidkhunthod and K. Faungnawakij, *Energy Convers. Manage.*, **134**, 188 (2017).
7. J. Fu, X. Lu and P. E. Savage, *ChemSusChem*, **4**, 481 (2011).
8. J. G. Immer, M. J. Kelly and H. H. Lamb, *Appl. Catal. A: Gen.*, **375**, 134 (2010).
9. A. Dragu, S. Kinayyigit, E. J. Garcia-Suarez, M. Florea, E. Stepan, S. Velea, L. Tanase, V. Colliere, K. Philippot, P. Granger and V. I. Parvulescu, *Appl. Catal. A: Gen.*, **504**, 81 (2015).
10. M. Snåre, I. Kubičková, P. Mäki-Arvela, D. Chichova, K. Eränen and D. Y. Murzin, *Fuel*, **87**, 933 (2008).
11. J. G. Na, B. E. Yi, J. K. Han, Y. K. Oh, J. H. Park, T. S. Jung, S. S. Han, H. C. Yoon, J. N. Kim, H. Lee and C. H. Ko, *Energy*, **47**, 25 (2012).
12. A. T. Madsen, E. Ahmed, C. H. Christensen, R. Fehrmann and A. Riisager, *Fuel*, **90**, 3433 (2011).
13. Y. X. Liu, X. J. Yang, H. Y. Liu, Y. H. Ye and Z. J. Wei, *Appl. Catal. B: Environ.*, **218**, 679 (2017).
14. M. Ojeda, N. Osterman, G. Drazic, L. F. Zilnik, A. Meden, W. Kwapinski, A. M. Balu, B. Likozar and N. N. Tusar, *Top. Catal.*, **61**, 1757 (2018).
15. J. C. Wang, L. Xu, R. F. Nie, X. L. Lyu and X. Y. Lu, *Fuel*, **265**, 11 (2020).
16. Z. H. Zhang, Q. W. Yang, H. Chen, K. Q. Chen, X. Y. Lu, P. K. Ouyang, J. Fu and J. G. G. Chen, *Green Chem.*, **20**, 197 (2018).
17. Z. H. Zhang, H. Chen, C. X. Wang, K. Q. Chen, X. Y. Lu, P. K. Ouyang and J. Fu, *Fuel*, **230**, 211 (2018).
18. Y. X. Liu, Y. J. Gu, Y. X. Hou, Y. Yang, S. G. Deng and Z. J. Wei, *Chem. Eng. J.*, **275**, 271 (2015).
19. Y. X. Liu, K. Zhou, M. Lu, L. C. Wang, Z. J. Wei and X. N. Li, *Ind. Eng. Chem. Res.*, **54**, 9124 (2015).
20. R. Ferrando, J. Jellinek and R. L. Johnston, *Chem. Rev.*, **108**, 845 (2008).
21. E. Roduner, *Chem. Soc. Rev.*, **35**, 583 (2006).
22. B. Al Alwan, S. O. Salley and K. Y. S. Ng, *Appl. Catal. A: Gen.*, **498**,

32 (2015).
23. H. P. Zhang, H. F. Lin and Y. Zheng, *Appl. Catal. B: Environ.*, **160**, 415 (2014).
24. S. Y. Xing, Y. Liu, X. C. Liu, M. Li, J. Y. Fu, P. F. Liu, P. M. Lv and Z. M. Wang, *Appl. Catal. B: Environ.*, **269**, 118718 (2020).
25. L. Q. Yang, K. L. Tate, J. B. Jasinski and M. A. Carreon, *ACS Catal.*, **5**, 6497 (2015).
26. T. L. Silva, A. Ronix, O. Pezoti, L. S. Souza, P. K. T. Leandro, K. C. Bedin, K. K. Beltrame, A. L. Cazetta and V. C. Almeida, *Chem. Eng. J.*, **303**, 467 (2016).
27. Z. Wei, J. Lou, C. Su, D. Guo, Y. Liu and S. Deng, *ChemSusChem*, **10**, 1720 (2017).
28. L. Perini, C. Durante, M. Favaro, V. Perazzolo, S. Agnoli, O. Schneider, G. Granozzi and A. Gennaro, *ACS Appl. Mater. Interfaces*, **7**, 1170 (2015).
29. K. S. Lakhi, D. H. Park, K. Al-Bahily, W. Cha, B. Viswanathan, J. H. Choy and A. Vinu, *Chem. Soc. Rev.*, **46**, 72 (2017).
30. Z. Wei, R. Pan, Y. Hou, Y. Yang and Y. Liu, *Sci. Rep.*, **5**, 15664 (2015).
31. Z. F. Shao, C. Li, X. Di, Z. H. Xiao and C. H. Liang, *Ind. Eng. Chem. Res.*, **53**, 9638 (2014).
32. S. A. Theofanidis, R. Batchu, V. V. Galvita, H. Poelman and G. B. Marin, *Appl. Catal. B: Environ.*, **185**, 42 (2016).
33. X. M. Tao, G. W. Wang, L. Huang, X. X. Li and Q. G. Ye, *Catal. Lett.*, **146**, 2129 (2016).
34. E. Hong, S. Bang, J. H. Cho, K. D. Jung and C. H. Shin, *Appl. Catal. A: Gen.*, **542**, 146 (2017).
35. X. Yue, S. Yi, R. Wang, Z. Zhang and S. Qiu, *Sci. Rep.*, **6**, 22268 (2016).
36. B. A. Rosen, E. Gileadi and N. Eliaz, *Catal. Commun.*, **76**, 23 (2016).
37. N. Ota, M. Tamura, Y. Nakagawa, K. Okumura and K. Tomishige, *ACS Catal.*, **6**, 3213 (2016).
38. Y. Takeda, M. Tamura, Y. Nakagawa, K. Okumura and K. Tomishige, *ACS Catal.*, **5**, 7034 (2015).
39. S. B. Liu, Y. Okuyama, M. Tamura, Y. Nakagawa, A. Imai and K. Tomishige, *Catal. Today*, **269**, 122 (2016).
40. K. H. Kang, U. G. Hong, Y. Bang, J. H. Choi, J. K. Kim, J. K. Lee, S. J. Han and I. K. Song, *Appl. Catal. A: Gen.*, **490**, 153 (2015).
41. A. Suknev, V. Zaikovskii, V. Kaichev, E. Paukshtis, E. Sadovskaya and B. Bal'zhinimaev, *J. Energy Chem.*, **24**, 646 (2015).
42. S. Oktay, Z. Kahraman, M. Urgen and K. Kazmanli, *Appl. Surf. Sci.*, **328**, 255 (2015).
43. Z. J. Wei, X. M. Zhu, X. S. Liu, H. Q. Xu, X. H. Li, Y. X. Hou and Y. X. Liu, *Chin. J. Chem. Eng.*, **27**, 369 (2019).
44. J. Asomaning, P. Mussone and D. C. Bressler, *J. Anal. Appl. Pyrolysis*, **105**, 1 (2014).
45. C. F. de Graauw, J. A. Peters, H. van Bekkum and J. Huskens, *Synthesis*, **1994**, 1007 (1994).
46. J. Vanderwaal, P. Kunkeler, K. Tan and H. Vanbekkum, *J. Catal.*, **173**, 74 (1998).
47. D. R. Vardon, B. K. Sharma, H. Jaramillo, D. Kim, J. K. Choe, P. N. Ciesielski and T. J. Strathmann, *Green Chem.*, **16**, 1507 (2014).
48. J. Fu, F. Shi, L. T. Thompson, X. Y. Lu and P. E. Savage, *ACS Catal.*, **1**, 227 (2011).
49. Z. H. Zhang, Z. Chen, X. Gou, H. Chen, K. Q. Chen, X. Y. Lu, P. K. Ouyang and J. Fu, *Ind. Eng. Chem. Res.*, **57**, 8443 (2018).
50. T. G. Kelly and J. G. Chen, *Chem. Soc. Rev.*, **41**, 8021 (2012).
51. W. Yu, M. D. Porosoff and J. G. Chen, *Chem. Rev.*, **112**, 5780 (2012).
52. M. Zhao, K. Yuan, Y. Wang, G. Li, J. Guo, L. Gu, W. Hu, H. Zhao and Z. Tang, *Nature*, **539**, 76 (2016).

Supporting Information

Design of low-loaded NiRe bimetallic catalyst on N-doped mesoporous carbon for highly selective deoxygenation of oleic acid to n-heptadecane

Zuojun Wei*,, Yuran Cheng*,**, Mengting Chen***, Yuhua Ye***, and Yingxin Liu***,†**

*Key Laboratory of Biomass Chemical Engineering of the Ministry of Education, College of Chemical and Biological Engineering, Zhejiang University, 38 Zheda Road, Xihu District, Hangzhou 310027, P. R. China
**Institute of Zhejiang University-Quzhou, 78 Jinhua Boulevard North, Quzhou 324000, P. R. China
***Research and Development Base of Catalytic Hydrogenation, College of Pharmaceutical Science, Zhejiang University of Technology, 18 Chaowang Road, Xiacheng District, Hangzhou 310014, P. R. China
(*Received 2 November 2021 • Revised 24 January 2022 • Accepted 27 January 2022*)

Table S1. Surface element scanning of Ni/NMC, Re/NMC and $Ni_{80}Re_{20}$/NMC catalysts by XPS

Catalyst	Elemental species	Binding energy (eV)	Content
$Ni_{80}Re_{20}$/NMC	Ni(0) $2p_{3/2}$	852.1	9%
	Ni(+2) $2p_{3/2}$	854.5	42%
	Ni(+2) $2p_{3/2}$ shakeup	860.5	49%
	Ni(0) $2p_{1/2}$	869.6	
	Ni(+2) $2p_{1/2}$	872.0	
	Ni(+2) $2p_{1/2}$ shakeup	878.0	
	Re(0) Re $4f_{7/2}$	40.3	26%
	Re(+3) Re $4f_{7/2}$	41.3	18%
	Re(+6) Re $4f_{7/2}$	45.1	56%
	Re(0) Re $4f_{5/2}$	42.7	
	Re(+3) Re $4f_{5/2}$	43.7	
	Re(+6) Re $4f_{5/2}$	47.6	
Ni/NMC	Ni(0) $2p_{3/2}$	851.8	15%
	Ni(+2) $2p_{3/2}$	854.2	51%
	Ni(+2) $2p_{3/2}$ shakeup	860.2	34%
	Ni(0) $2p_{1/2}$	869.3	
	Ni(+2) $2p_{1/2}$	871.7	
	Ni(+2) $2p_{1/2}$ shakeup	877.7	
Re/NMC	Re(0) Re $4f_{7/2}$	40.6	12%
	Re(+3) Re $4f_{7/2}$	41.6	22%
	Re(+4) Re $4f_{7/2}$	42.5	13%
	Re(+6) Re $4f_{7/2}$	45.3	53%
	Re(0) Re $4f_{5/2}$	43.0	
	Re(+3) Re $4f_{5/2}$	44.0	
	Re(+4) Re $4f_{5/2}$	44.9	
	Re(+6) Re $4f_{5/2}$	47.8	

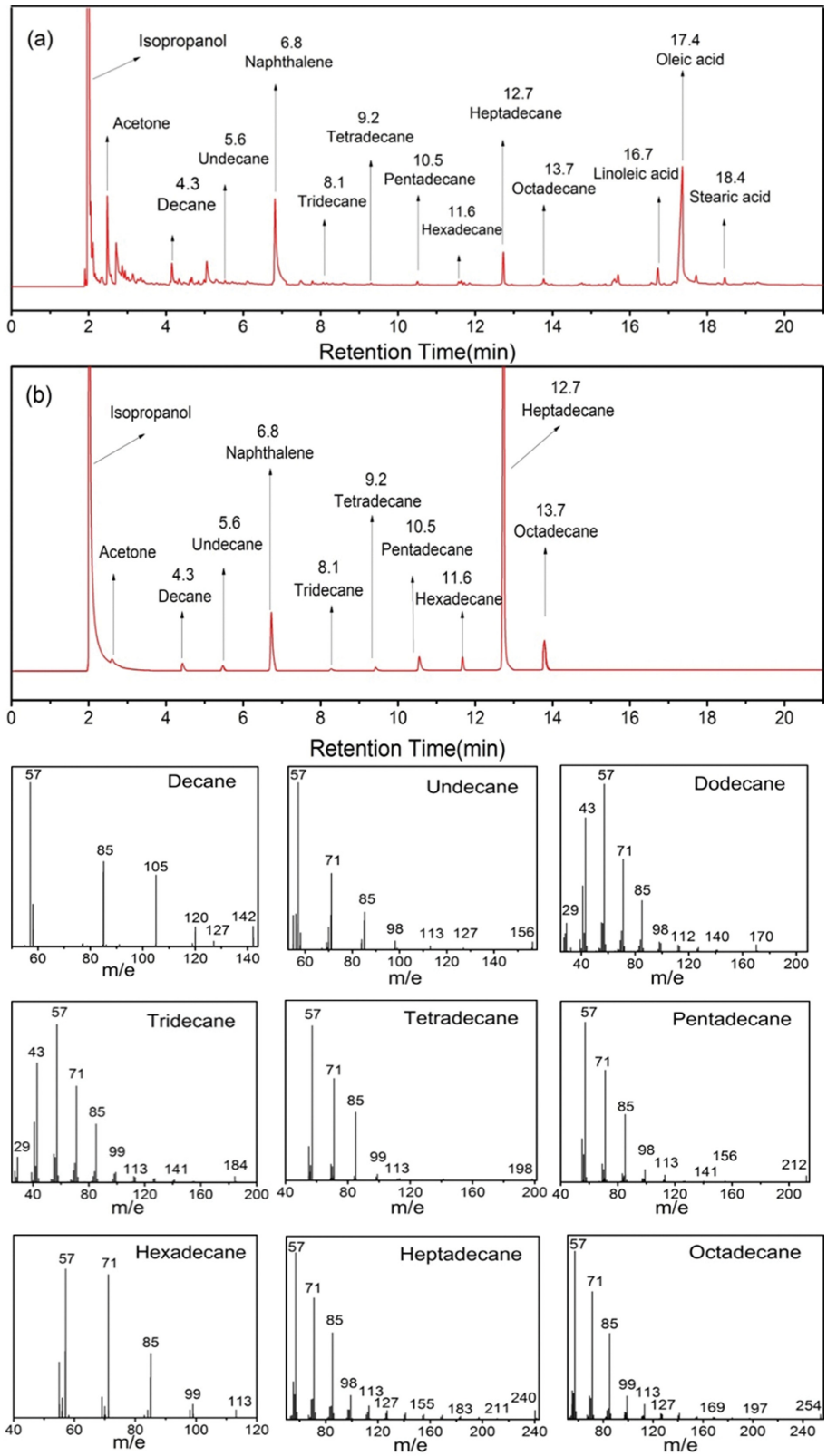

Fig. S1. GC-MS spectra of the products of oleic acid deoxygenation over (a) $Ni_{50}Re_{50}/SiO_2$ and (b) $Ni_{50}Re_{50}$/NMC catalysts.

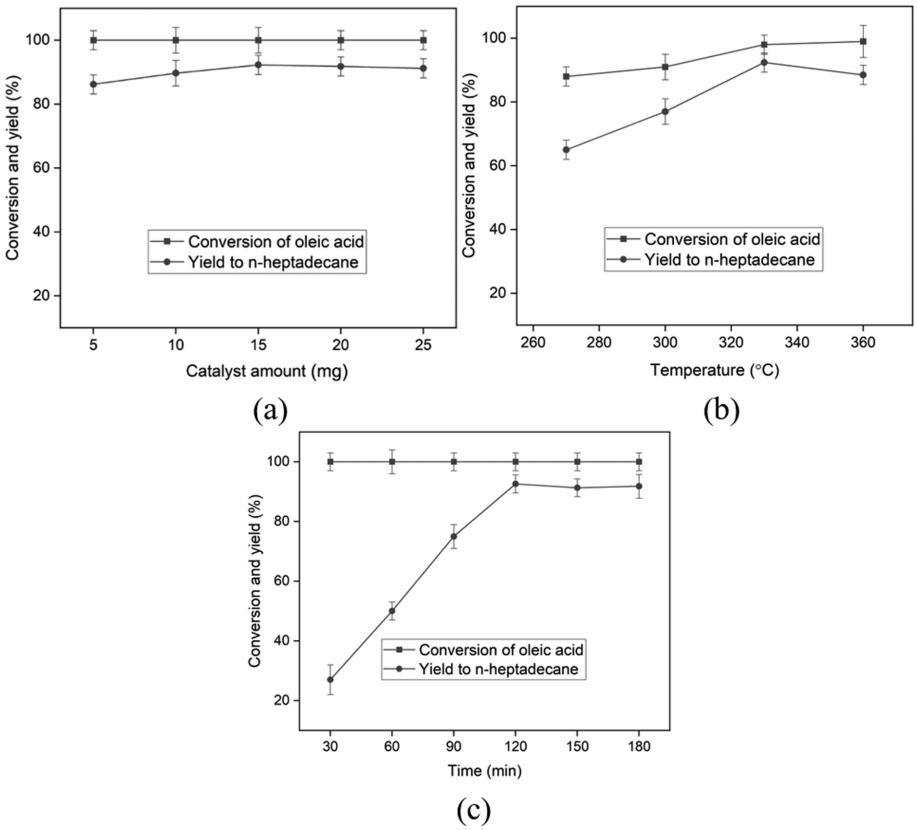

Fig. S2. Optimization of reaction conditions for the deoxygenation of oleic acid over $Ni_{80}Re_{20}$/NMC catalyst. (a) Amount of catalyst (reaction temperature, 330 °C; reaction time, 2 h); (b) reaction temperature (catalyst, 15 mg; reaction time, 2 h); (c) reaction time (catalyst, 15 mg; reaction temperature, 330 °C). Typical reaction conditions: oleic acid, 50 mg; isopropanol, 1 ml. ■ Conversion of oleic acid; ● Yield to n-heptadecane.

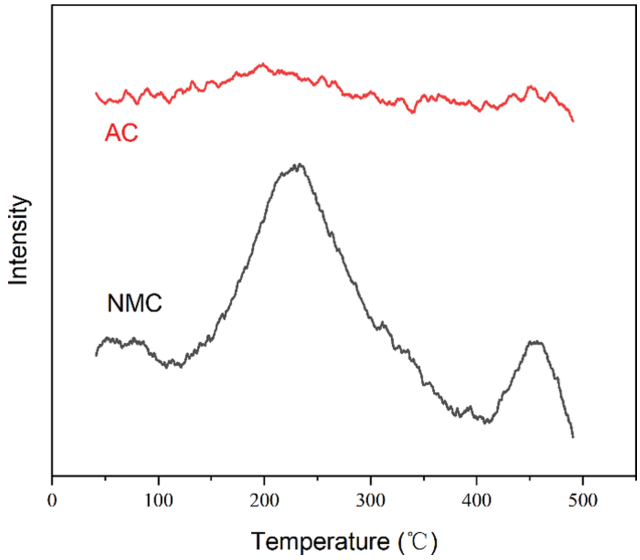

Fig. S3. CO_2-TPD profiles of the as-prepared NMC and commercial AC (activated carbon) supports.

Table S2. Reduction potential of hydrogen donors

Reductant state		Oxygen state		$-\Delta_{red}H^0$ (kJ·mol^{-1})
Substance	Δ_fH^0 (kJ·mol^{-1})	Substance	Δ_fH^0 (kJ·mol^{-1})	
Formic acid (l)	−425	Carbon dioxide	−393.5	31.5
Isopropanol (l)	−318.1	Acetone (l)	−248.2	69.9
Ethanol (l)	−277.6	Acetaldehyde (l)	−192.2	85.4
Methanol (l)	−239.2	Formaldehyde (g)	−108.6	130.6
Water (l)	−239.2	Oxygen (g)	0	239.2
tert-Butanol (l)	334.7	-	-	-

Standard enthalpies of formation of the substances are taken from Lide [1].

Table S3. Deoxygenation of oleic acid over NiRe catalysts in mixed solvent

Entry	Catalyst	Tetradecane (ml)	Isopropanol (ml)	Conversion (%)	N-heptadecane yield (%)
1	$Ni_{50}Re_{50}/\gamma$-Al_2O_3	0.9	0.1	>99	10.8
2	$Ni_{50}Re_{50}/\gamma$-Al_2O_3	0.5	0.5	83	21.1
3	$Ni_{80}Re_{20}$/NMC	0.9	0.1	>99	45.0
4	$Ni_{80}Re_{20}$/NMC	0.5	0.5	>99	68.6

Reaction conditions: oleic acid, 50 mg; tetradecane+isopropanol, 1 ml; catalyst, 15 mg; reaction temperature, 330 °C; reaction time, 2 h.

The Meerwein-Ponndorf-Verley-Oppenauer reaction is a kind of displacement reaction between an alcohol and an aldehyde/ketone. To determine the reduction ability of an alcohol and the oxidation ability of an aldehyde/ketone, a reduction potential $-\Delta_{red}H^0$ was introduced, which is defined as the difference in enthalpy of formation between the alcohol and the corresponding aldehyde/ketone [2,3]. An alcohol having a lower $-\Delta_{red}H^0$ therefore corresponds to a higher ability for delivering H atoms and getting oxidized, which is used herein to specify the ability to supply hydrogen for the following C=C addition reactions.

Based on this theory, water can be viewed as reductant alcohol, which can deliver H atoms and get oxidized to oxygen. The $-\Delta_{red}H^0$ of water can then be estimated as the difference between Δ_fH^0 (water) and Δ_fH^0 (oxygen), i.e. 239.2 kJ·mol^{-1}. Formic acid, which delivers hydrogen atoms, while is oxidized to CO_2. So the $-\Delta_{red}H^0$ of formic acid can then be estimated as the difference between Δ_fH^0 (formic acie) and Δ_fH^0 (carbon dioxide), i.e. 31.5 kJ·mol^{-1}.

REFERENCES

1. D. R. Lide, *CRC handbook of chemistry and physics*, 84 Ed., CRC press (2003-2004).
2. C. F. de Graauw, J. A. Peters, H. van Bekkum and J. Huskens, *Synthesis*, **1994**(10), 1007 (1994).
3. J. Vanderwaal, P. Kunkeler, K. Tan and H. Vanbekkum, *J. Catal.*, **173**(1), 74 (1998).